Self-Assembly and Paclitaxel Loading Capacity of Cellulose-*graft*-poly(lactide) Nanomicelles

Yanzhu Guo,[†] Xiaohui Wang,*[,†] Xuancai Shu,[†] Zuguang Shen,[†] and Run-Cang Sun*[,†,‡]

[†]State Key Laboratory of Pulp and Paper Engineering, South China University of Technology, Guangzhou 510640, China
[‡]Institute of Biomass Chemistry and Technology, Beijing Forestry University, Beijing 100083, China

ABSTRACT: A series of amphiphilic cellulose-based graft copolymers (MCC-*g*-PLA) with various molecular factors were synthesized in ionic liquid BmimCl and characterized by FT-IR, ^{1}H NMR, ^{13}C NMR, XRD, and TGA. Their solubility in a variety of solvents was compared. The prepared MCC-*g*-PLA copolymers can self-assemble into spherical nanomicelles (10−50 nm) in aqueous solution. The self-assembly behaviors of the MCC-*g*-PLA copolymers were systematically investigated by fluorescence probe. Furthermore, the hydrophobic antitumor drug paclitaxel (PTX) was successfully encapsulated into the MCC-*g*-PLA micelles. The drug encapsulation efficiency and loading content were found to be as high as 89.30% (w/w) and 4.97%, respectively. Results in this study not only suggest a promising cellulose-based antitumor drug carrier but also provide information for property-directed synthesis of the cellulose graft PLA copolymers.

KEYWORDS: cellulose, ʟ-lactide, biodegradable, nanomicelle, PTX

■ INTRODUCTION

Over the past decades, polymeric micelles formed by self-assembly of amphiphilic block copolymers in aqueous solution have been extensively investigated and applied in antitumor drug delivery system, due to their favorable characteristics of solubilization, long circulation, low toxicity, enhanced drug bioavailability, reduced side effects of drugs, etc.[1−5] The structure of polymeric micelles is characterized by a hydrophobic core and a hydrophilic exterior, which spontaneously forms above the critical micelle concentration (CMC) of the polymers.[6,7] The loading ability of micelles commonly relies on physical encapsulation during the assembly process, whereby hydrophobic drug molecules can be sequestered in the hydrophobic core. To date, a large number of polymers have been prepared to form self-assembled micelles, most of which are linear block copolymers composed by synthetic main chains, such as poly(ethylene glycol) (PEG),[8] poly(*N*-vinyl-2-pyrrolidone) (PVP),[9] poly(vinyl alcohol) (PVA)[10] et al., and hydrophobic segments, such as vinylic polymers,[11] polyester,[12,13] poly(amino acid) et al.[14−17] Recently, micelles formed from comb-like graft copolymers of natural renewable materials, for example, polysaccharides, are attracting increasing interest because of their inherent biodegradability and biocompatibility.[18]

Cellulose is one of the most abundant renewable polysaccharides in nature. It is a promising "green" material owing to its unique properties such as nontoxicity, recyclability, and low cost. The functionalization and value-added utilization of cellulose is always an important topic in the field of agriculture and food research.[19,20] Grafting hydrophobic segments to the cellulose backbone would give rise to amphiphilic copolymers, which can form self-assembled micelles for food applications.[20] Many hydrophobic segments have been successfully grafted onto cellulose or cellulose derivatives, among which grafting biodegradable and biocompatible aliphatic polyesters onto cellulose are of most

concern.[21−27] Poly(ʟ-lactide) (PLA), as one FDA-approved aliphatic polyester, has been widely used as a biodegradable structural material. In previous studies, the grafting copolymerization of PLA onto cellulose derivatives such as cellulose acetate, ethyl cellulose, and hydroxyethyl or hydroxypropyl cellulose was successfully carried out.[28−30] Unfortunately, the biodegradability of these highly modified cellulose derivatives is still a problem.[31] Therefore, directly grafting biodegradable polymers onto the cellulose backbone will be more favorable because the copolymers obtained from PLA and cellulose will combine the advantages of both and will be completely biodegradable under natural conditions, in addition to their improved performance.[32] However, it is also well-known that cellulose is insoluble in common solvents due to its specific molecular structure, which causes a great difficulty in performing controlled graft reaction of cellulose.

Ionic liquids (ILs), which are often regarded as intrinsically "green" due to their negligible vapor pressure, have been discovered to be excellent solvents for cellulose.[33,34] Two typical ILs (1-*n*-butyl-3-methylimidazolium chloride (BmimCl)[35] and 1-*n*-alkyl-3-methylimidazolium chloride (AmimCl)[36]) have been utilized to dissolve cellulose. Dong et al.[37] and Yan et al.[32] prepared cellulose-*g*-PLA copolymers by ring-opening graft copolymerization (ROP) of ʟ-lactide (LA) onto cellulose in AmimCl and studied their properties. It is noteworthy that cellulose-*g*-PLA is significantly different from conventional linear block copolymers not only due to their branched architecture but also owing to their rigid, crystalline main chain. When micelles formed from such copolymers are used as drug carriers, many performance-related issues must be addressed, including their stability, shape, size and size

distribution, and drug-loading capacity. To a large extent, these properties of polymeric micelles are determined by the architecture of polymers. However, very little is known about the polymer architecture−property relationships of cellulose-*g*-PLA.

In this paper, a series of microcrystalline cellulose-*graft*-PLA (MCC-*g*-PLA) copolymers with various structural factors, including grafting ratio, hydrophobic chain length, and molecular weight, were prepared by the homogeneous graft copolymerization of cellulose and LA in a new ionic liquid, BmimCl. The chemical structures and physical properties of MCC-*g*-PLA copolymers were characterized with FT-IR, ^{1}H NMR, ^{13}C NMR, XRD, and TGA. The solubility of these copolymers in a variety of organic solvents and water was evaluated. The self-assembling behaviors and the micelle properties characterized by the CMC, morphology, size, and size distribution were systematically investigated in terms of different structural factors of MCC-*g*-PLA copolymers. Moreover, the antitumor drug loading and solubilizing capacities of the MCC-*g*-PLA micelles were studied using paclitaxel (PTX) as a model drug, and the polymer architecture−property relationship was discussed.

■ MATERIALS AND METHODS

Materials. MCC with a degree of polymerization (DP) of 200 (Sinopharm Chemical Reagent Co., Ltd., Shanghai, China) and BmimCl with a purity of 99% (Cheng Jie Chemical Co., Ltd., Shanghai, China) were first dried in a vacuum for 48 h at 45 °C before use. L-Lactide (L-LA) with a purity of 99.5% was purchased from Jinan Daigang Biomaterial Co., Ltd. Stannous octanoate (Sn(Oct)$_2$) was provided by Aladdin-reagent Inc. All other solvents were of analytical reagent grade and directly used without further purification.

Synthesis of MCC-*g*-PLA Copolymers. Typically, MCC (1.0 g) was added to 14.3 g of BmimCl in a 50 mL dried three-neck flask. The mixture was then placed into an oil bath and heated on a hot plate with vigorous magnetic stirring at 80 °C for 2 h under nitrogen atmosphere. After the complete dissolution of MCC in BmimCl, the monomer of L-LA and 0.2 wt % Sn(Oct)$_2$ as the catalyst were slowly added into the solution, and the ring-opening graft polymerization was carried out at 110 or 130 °C under N$_2$ atmosphere with vigorous stirring for 8 h. After cooling to room temperature, the resultant copolymer was isolated by precipitating the reaction mixture into 250 mL of isopropanol and washed five times with isopropanol to remove unreacted monomer, residual catalyst, and BmimCl. Subsequently, the polymer was suspended in 25 mL of dichloromethane and magnetically stirred at room temperature for 72 h to dissolve homo-PLA, which could be formed during the grafting reaction. Finally, the copolymers was filtered through a glass filter (0.45 um) and washed several times with more dichloromethane to confirm the complete remove of any free homopolymer. The final product was dried in a vacuum for 48 h at 60 °C.

Characterization of MCC-*g*-PLA Copolymers. FT-IR spectra were collected on a Bruker spectrometer (TENSOR27, Switzerland). ^{1}H NMR and ^{13}C NMR spectra were obtained with a Bruker AV-III 400 M spectrometer (Germany) at 100 MHz using DMSO-d_6 as solvent and tetramethysilane (TMS) as internal standard. The molecular weight (M_w) and polydispersity of the copolymers were determined by a gel permeation chromatography (GPC) instrument equipped with a PL aquagel-OH 50 column (300 × 7.7 mm, Polymer Laboratories Ltd.) and a differential refractive index detector (RID). The measurements were performed with 5 mM sodium phosphate buffer (pH 7.5) containing 0.02 N NaCl as the eluent at a flow rate of 0.5 mL/min at 30 °C and a series of PL pullulan polysaccharide standards (M_w of 783, 12200, 100000, and 1600000, Polymer Laboratories Ltd.) for the calibration of the columms. X-ray diffraction (XRD) was determined by a D/max-IIIA X-ray diffractometer, in which the high-intensity monochromatic nickel-filtered Cu Kα

radiation was generated at 40 kV and 40 mA. Samples were scanned at a speed of 1°/min, range from 2θ = 5−45° with step size of 0.04° at room temperature. The thermal stability of the MCC-*g*-PLA copolymers was evaluated using thermogravimetric analysis (TGA) (TGA Q500, TA, USA). Samples of approximately 5 mg weight were heated in an aluminum crucible to 600 °C at a heating rate of 10 °C min^{-1} while the apparatus was continually flushed with a nitrogen flow of 30 mL min^{-1}.

The solubilities of MCC-*g*-PLA copolymers in dimethyl sulfoxide (DMSO), tetrahydrofuran (THF), dimethyl formamide (DMF), water, and hexane were evaluated in this experiment. Ten milligrams of each sample was placed in a test tube with 4 mL of each solvent. After mixing with a vortex mixer and a subsequent ultrasonic treatment, the mixture was stored at room temperature for 5 days and observed visually.

Preparation and Characterization of MCC-*g*-PLA Micelles. In a typical experiment, 20 mg of MCC-*g*-PLA copolymers was dissolved in 1 mL of DMSO, and then the solution was slowly dropped into 2 mL of deionized water with vigorous stirring. The mixture was transferred to a dialysis bag (MWCO = 3000) and dialyzed against plenty of deionized water for 24 h (the deionized water was refreshed every 6 h). After the DMSO was completely removed, the dialyzed solutions were adjusted to a definite concentration for subsequent characterization.

The size and size distribution (PDI) of MCC-*g*-PLA micelles were determined by dynamic light scattering (DLS) on a Zetasizer 3000 HS instrument at 90° scattering angle at 25 °C. A semiconductor laser diode (30 mW, 633 nm) was the light source. All analyses were performed with six duplicates, and the results were recorded as the statistical average values. Transmission electron microscopy (TEM) was performed using a JEM-2100 operated at an accelerating voltage of 200 kV. A drop of the sample with a concentration of 0.5 mg/mL was placed on the copper grids coated with carbon film and stained with phosphotungstic acid (2%, w/w) for 3 min before testing.

Determination of CMC. First, the copolymer micelle solutions with a series of concentrations from 0.001 to 2 mg/mL were prepared according to the above membrane dialysis method. The aliquots of pyrene stock solution (6.0×10^{-5} M in THF, 50 μL) were added to containers, and the solvent THF was allowed to evaporate. The micelle solutions (5 mL) with different concentrations were then transferred to the containers with pyrene residues to make the final concentration of pyrene to be 6.0×10^{-7} M. The combined solutions of pyrene and copolymers were equilibrated at room temperature in the dark for 24 h before measurement.

Fluorescence spectra were obtained using a fluorescence spectrophotometer (Jobin-Yvon Fluorolog Tau-3 system) at room temperature. The emission spectra were scanned from 360 to 550 nm with the excitation wavelength of 339 nm. The intensity ratio (I_1/I_3) of the first band (375 nm, I_1) to the third band (386 nm, I_3) from the emission spectra was analyzed as a function of copolymer concentration. The first point of inflection of intensity ratio (I_1/I_3) against polymer concentration was taken as the CMC.

Antitumor Drug Loading Capacity of MCC-*g*-PLA Micelles. First, 5 mL of MCC-*g*-PLA micelle solution (1 mg/mL) was prepared according to the membrane dialysis method. Subsequently, a determined amount of PTX dissolved in methanol (polymer/drug = 20:1) was slowly added into this micelle solution followed by 30 min of ultrasonication at room temperature to remove methanol. The solution was further ultrasonicated for 5 min (active every 1 s for a 3 s duration with the power of 100 W) in an ice bath by a probe-type ultrasonicator (Bandelin SONOPULS, Germany). The resultant PTX-loaded micelles solution was centrifuged at 10000g for 15 min to remove unloaded PTX precipitates, and the supernatant was filtered through a 1 μm membrane filter. The drug loading content (DL, %) and encapsulation efficiency (EE, %) of paclitaxel in MCC-*g*-PLA micelles were determined by using a UV−vis spectrophotometer at 227 nm according to the following equations:[38,39]
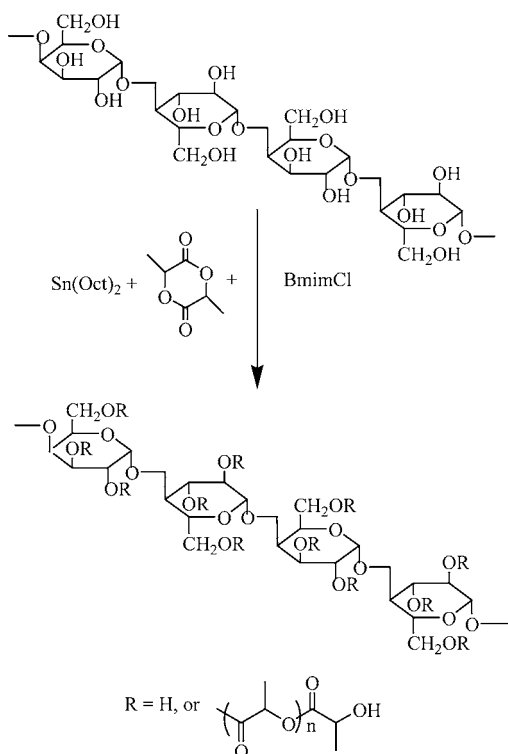
$$DL\ (\%) = (wt\ of\ loaded\ drug/wt\ of\ polymer) \times 100\%$$

$$EE \, (\%) = (\text{wt of loaded drug/wt in feed}) \times 100\%$$

RESULTS AND DISCUSSION

Synthesis and Characterization of MCC-*g*-PLA Copolymers. A series of amphiphilic cellulose-*g*-PLA copolymers

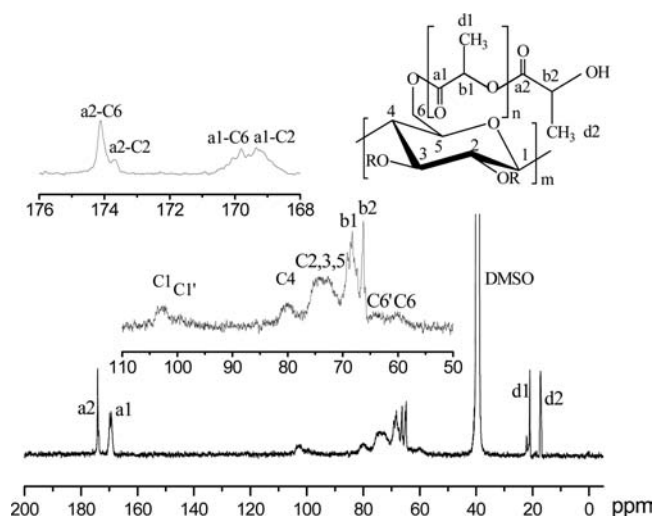**Scheme 1. Synthesis of MCC-*g*-PLA Using Sn(Oct)$_2$ as a Catalyst in Ionic Liquid BmimCl**

with different molecular factors were prepared in IL BmimCl by ring-opening polymerization (ROP) of L-lactide onto cellulose. In the reaction, Sn(Oct)$_2$ was applied as an assistant catalyst to co-initiate the ROP of L-lactide with the hydroxyl group of cellulose. The expected structure of MCC-*g*-PLA is shown in Scheme 1. It was well-known that the strong inter- and intramolecular hydrogen bonds in cellulose are the major reason for its insolubility in water and common organic solvents. As a much stronger hydrogen bond acceptor, ILs could interact with the hydroxyl groups of cellulose and result in efficient dissolving of cellulose at comparably mild conditions.[40] Moreover, ILs could readily dissolve the hydrophobic grafting molecules, such as polyester; thus, the grafting reaction could be performed in a homogeneous system.
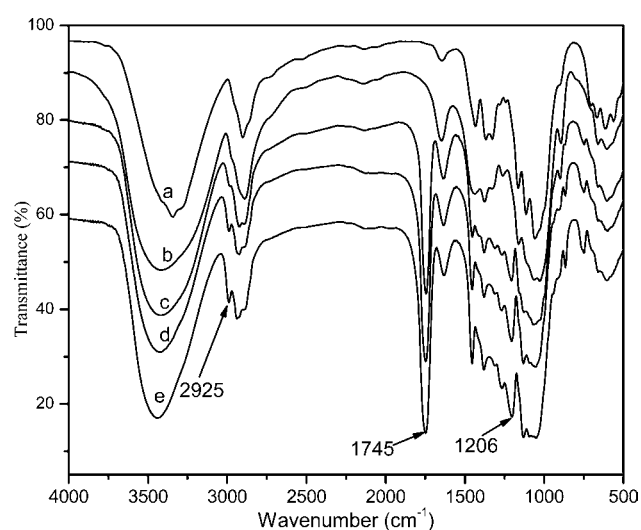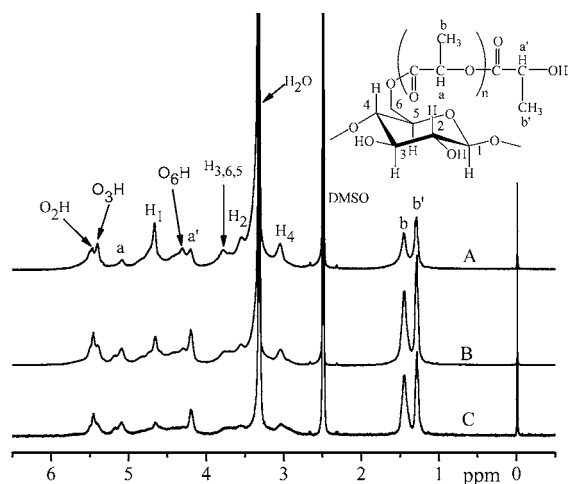
Figure 1. ^{13}C NMR (DMSO-d_6) spectra of MCC-*g*-PLA copolymers (MCC-*g*-PLA$_{1.43}$).

Figure 2. FT-IR spectra of cellulose and its derivatives: (a) cellulose; (b) Reg-cellulose; (c) MCC-*g*-PLA$_{0.55}$; (d) MCC-*g*-PLA$_{0.99}$; (e) MCC-*g*-PLA$_{1.43}$.

Generally, for branched copolymers, graft ratio and M_w were considered to be the controlling factors that affect the micelle properties.[41] Previous studies have revealed that the reacting temperature is a key factor determining the degradation degree of cellulose during the modification reaction in ILs. Therefore, reactions at different temperatures were carried out to control

Table 1. Synthesis Detail of Homogeneous Graft PLA onto Cellulose in BmimCl

| sample	AGU/L-LA^a	T (°C)	DP$_{PLA}$^{b}	MS^b	DS^b	W_{PLA}^{b} (%)	M_n^{c}	M_w^{c}	M_w/M_n^{c}
1	1:1	130	1.74	0.87	0.50	27.88	6275	10844	1.73
2	1:2	130	1.84	1.77	0.96	44.03	9681	16720	1.73
3	1:4	130	2.16	2.96	1.37	56.81	11068	19685	1.78
4	1:1	110	2.00	1.09	0.55	32.63	23909	50972	2.13
5	1:2	110	1.96	1.68	0.85	42.75	25691	55216	2.15
6	1:3	110	2.23	2.21	0.99	49.55	30821	62508	2.03
7	1:4	110	2.22	3.17	1.43	58.49	38689	82464	2.13
8	1:6	110	2.39	4.78	2.00	67.99			

^{a}Molar ratio. ^{b}Determined by ^{1}H NMR. ^{c}Determined by GPC.

Figure 3. ^1H NMR (DMSO-d_6) spectra of MCC-*g*-PLA copolymers: (A) MCC-*g*-PLA$_{0.55}$; (B) MCC-*g*-PLA$_{0.99}$; (C) MCC-*g*-PLA$_{1.43}$.

**Table 2. Dissolving Ability of MCC-*g*-PLA Copolymers in Water and Organic Solvents**[a]

sample[b]	DMSO	DMF	H$_2$O	THF	hexane
MCC-*g*-PLA$_{0.50}$	+++	+++	+++	−	−
MCC-*g*-PLA$_{0.96}$	+++	+++	+++	−	−
MCC-*g*-PLA$_{1.37}$	+++	+++	+++	−	−
MCC-*g*-PLA$_{0.55}$	+++	+++	+++	−	−
MCC-*g*-PLA$_{0.85}$	+++	+++	+++	−	−
MCC-*g*-PLA$_{0.99}$	+++	+++	+++	−	−
MCC-*g*-PLA$_{1.43}$	+++	+++	+++	−	−
MCC-*g*-PLA$_{2.00}$	+++	+++	−	−	−

[a] +++, dissolving; −, undissolving. [b] MCC-*g*-PLA$_{0.50}$ means that the DS of PLA is 0.50.
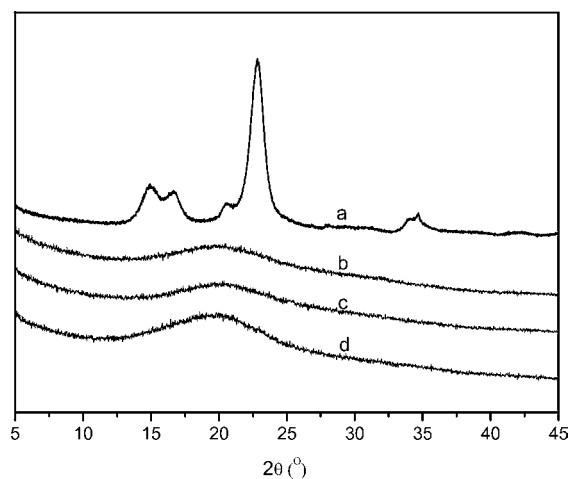
Figure 4. Wide-angle X-ray diagrams of cellulose and its derivatives: (a) cellulose; (b) MCC-*g*-PLA$_{0.55}$; (c) MCC-*g*-PLA$_{0.99}$; (d) MCC-*g*-PLA$_{1.43}$.

the M_w of MCC-*g*-PLA graft copolymers in this study. MCC-*g*-PLA graft copolymers with various grafting ratios and PLA side chain lengths were synthesized by adjusting the molar ratios of L-LA monomer to cellulose, and the synthesis details are presented in Table 1. The chemical structure of the MCC-*g*-PLA copolymers was characterized by ^1H NMR, ^{13}C NMR, FT-IR, and GPC analysis.
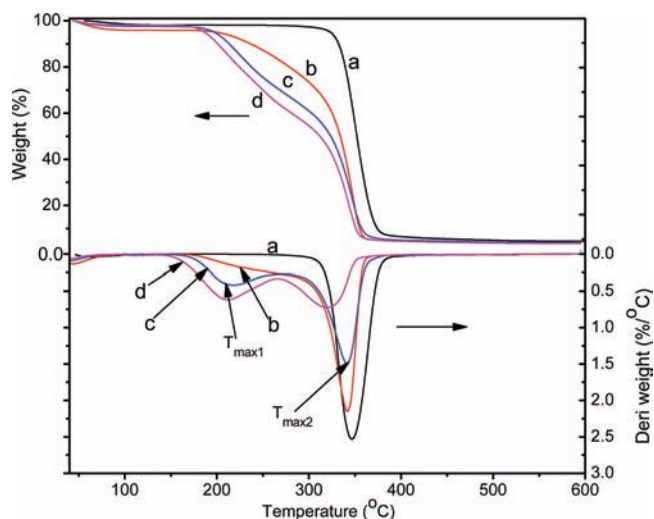

Figure 5. TG and DTG curves of cellulose and its derivatives: (a) cellulose; (b) MCC-*g*-PLA$_{0.55}$; (c) MCC-*g*-PLA$_{0.99}$; (d) MCC-*g*-PLA$_{1.43}$.

The ^{13}C NMR spectrum of MCC-*g*-PLA copolymers is shown in Figure 1. The carbons of the cellulose backbone appeared at 103.0, 70.9−76.4, 79.9, and 60.1 ppm, corresponding to C1, C2, 3, 5, C4, and C6 in anhydrous glucose units (AGU), respectively. The chemical shifts of C1 (103.0 ppm) and C1′ (99.6 ppm) corresponded to the C1 carbons adjacent to C2 bearing unsubstituted and substituted hydroxyl groups, respectively. Accordingly, C6 (60.1 ppm) and C6′ (63.7 ppm) were ascribed to the C6 carbons bearing unsubstituted and substituted hydroxyl groups, respectively. This result indicated that the hydroxyl groups of AGU in native cellulose were partially substituted. In addition, the spectra of cellulose-*g*-PLA gave a series of extra peaks, which were attributed to the carbons of PLA side chains. The peaks appearing at 68.4, 66.3, 21.1, and 17.3 ppm were ascribed to b1, b2, d1, and d2 (indexed in Figure 1) of ring-opened L-LA, respectively, whereas the two peaks at chemical shifts of 174.1 and 169.8 ppm were attributed to the carbonyl carbons of the repeating and ending unit of PLA side chains, respectively. Furthermore, in the magnified spectrum from 168 to 176 ppm, there were two peaks (174.1 and 173.7 ppm) belonging to the carbonyl carbons of a2 that could be assigned to the *O*-lactyl carbonyl carbons in C6 and C2 positions, respectively.[27,32] The carbonyl carbons of a1 in the PLA side chain were divided into two peaks (a1-C6, 169.8; a1-C2, 169.3 ppm), which also demonstrates that the LA molecule grafts at different positions of AGU.

The FT-IR spectra of MCC and its grafted derivatives are shown in Figure 2. Compared with the FT-IR spectra of MCC, the spectra of obtained MCC-*g*-PLA copolymers had new absorption peaks at around 1206, 1745, and 2925 cm^{-1} attributed to the symmetric C−O−C, carbonyl stretch, and CH$_3$ stretch vibrations of the PLA grafts, respectively. To confirm the signals at 1745 and 2925 cm^{-1} originate from the PLA grafted onto cellulose but not from the homo-PLA mixed with cellulose, a sample of regenerated cellulose (Reg-cellulose) was prepared by stirring a mixture of cellulose and L-lactide in BmimCl at 130 °C for 8 h and then removing homo-PLA by dichloromethane extraction. The FT-IR spectrum of Reg-cellulose indicated that ungrafted homo-PLA can be completely removed by dichloromethane extraction. Therefore, it was

3903

dx.doi.org/10.1021/jf3001873 | *J. Agric. Food Chem.* 2012, 60, 3900−3908

Table 3. Hydrodynamic Size and Size Distribution of MCC-*g*-PLA Micelles before and after Loading PTX

	blank micelles		PTX-loaded micelles	
sample	particle size (nm)	PDI	particle size (nm)	PDI
MCC-*g*-PLA$_{0.50}$	51.35 ± 3.27	0.44 ± 0.02	129.26 ± 1.69	0.31 ± 0.06
MCC-*g*-PLA$_{0.96}$	9.19 ± 1.96	0.35 ± 0.01	135.54 ± 5.42	0.42 ± 0.09
MCC-*g*-PLA$_{1.37}$	6.86 ± 0.95	0.57 ± 0.04	96.95 ± 3.82	0.27 ± 0.05
MCC-*g*-PLA$_{0.55}$	43.98 ± 2.26	0.35 ± 0.10	166.72 ± 3.75	0.24 ± 0.03
MCC-*g*-PLA$_{0.85}$	18.56 ± 3.11	0.32 ± 0.09	133.90 ± 4.51	0.25 ± 0.01
MCC-*g*-PLA$_{0.99}$	16.65 ± 0.25	0.33 ± 0.11	126.93 ± 1.27	0.33 ± 0.02
MCC-*g*-PLA$_{1.43}$	13.27 ± 2.17	0.42 ± 0.08	109.49 ± 5.96	0.39 ± 0.07
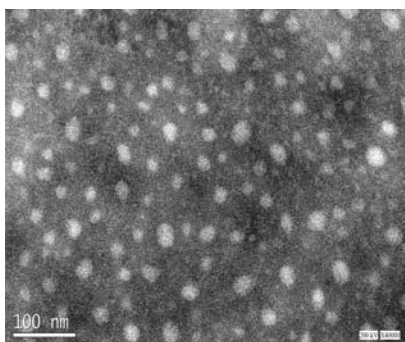
Figure 6. TEM micropicture of micelles of MCC-*g*-PLA copolymers (MCC-*g*-PLA$_{1.43}$).

Figure 7. (a) Pyrene emission spectra of MCC-*g*-PLA solutions (MCC-*g*-PLA$_{1.43}$, excitation wavelength of 339 nm). (b) Intensity ratio (I_{375}/I_{386}) of the pyrene emission spectra versus the log concentration of MCC-*g*-PLA copolymers (MCC-*g*-PLA$_{1.43}$).
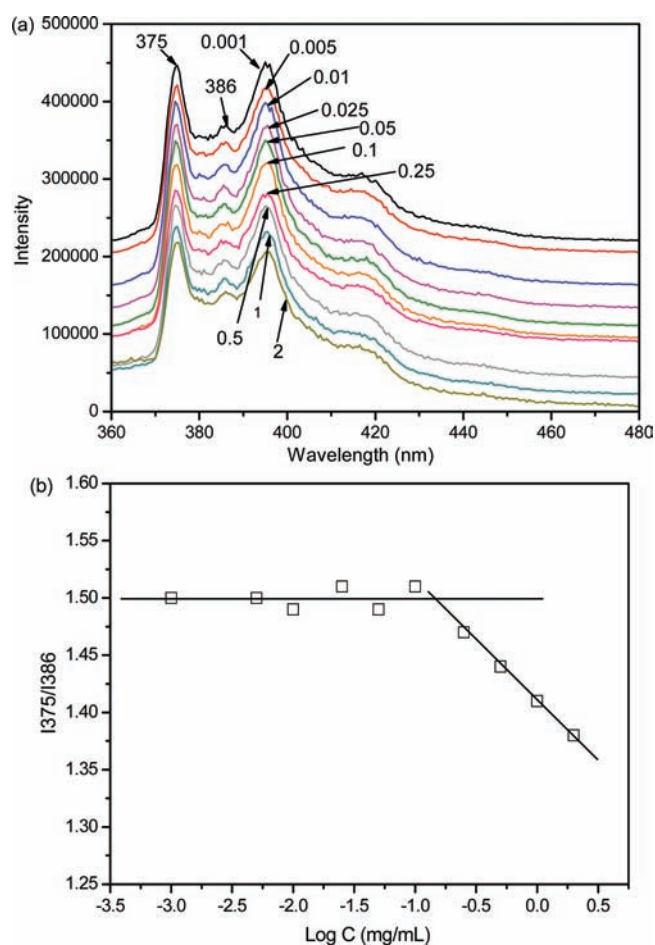
believable that the ring-opening graft copolymerization of L-LA onto cellulose backbone was successful. It was also observed that the copolymers exhibit enhanced absorptions at 1206, 1745, and 2925 cm^{-1} with increasing feed ratio of L-lactide to cellulose, which meant the grafting degree could be controlled by varying the feed ratio of LL-lactide to cellulose, as is further confirmed by the following ^{1}H NMR analysis results.

The ^{1}H NMR spectra of MCC-*g*-PLA with various DS values is shown in Figure 3. The resonance peaks derived from the protons of H$_1$, H$_{3,\,6,\,5}$, H$_2$, and H$_4$ in the AGU units of cellulose appeared at 4.66, 3.77, 3.55, and 3.05 ppm, respectively. The signals at 5.46, 5.40, and 4.31 ppm were ascribed, respectively, to the H-2, H-3, and H-6 protons of residual hydroxyl in cellulose. The new peaks at 1.45 and 1.29 ppm corresponded to the internal and terminal methyl protons (H$_b$ and H$_{b'}$) of PLA side chain, respectively, whereas the chemical shifts at 5.09 and 4.20 ppm were assigned to the internal and terminal methine protons (H$_a$ and H$_{a'}$) of PLA side chain, respectively. On the basis of the above peak assignments, the microstructures of MCC-*g*-PLA copolymers were analyzed in detail through calculations with the peak intensity in ^{1}H NMR spectra. Using the methods of the literature,[37,42] the structural factors of MCC-*g*-PLA copolymers were estimated with the following equations:

$$MS = \frac{\text{lactyl units}}{\text{anhydroglucose units}} = \frac{I_{(b+b')}/3}{I_{(O_2H+O_3H+O_6H)}/3} \quad (1)$$

$$DP_{PLA} = \frac{MS}{DS} = \frac{I_b}{I_{b'}} + 1 \quad (2)$$

$$DS = \frac{\text{terminal lactyl units}}{\text{anhydroglucose units}} = \frac{I_{b'}/3}{I_{(O_2H+O_3H+O_6H)}/3} \quad (3)$$

$$W_{PLA} = \frac{72MS}{162 + 72MS} \times 100\% \quad (4)$$

where DP$_{PLA}$, MS, DS, and W_{PLA} are the degree of polymerization of PLA (DP$_{PLA}$), the molar substitution of PLA (MS), the degree of substitution of PLA (DS), and the weight content of PLA side chains (W_{PLA}), respectively. The 72 and 162 g mol^{-1} in eq 3 are the molecular weights of L-LA monomer and cellulose repeating unit, respectively. The calculated values of these structural factors for synthesized MCC-*g*-PLA copolymers are presented in Table 1.

According to the results of Table 1, the PLA grafting ratio in terms of MS and W_{PLA} increased with the increasing amount of L-LA in-feed at the same reaction temperature. In addition, the
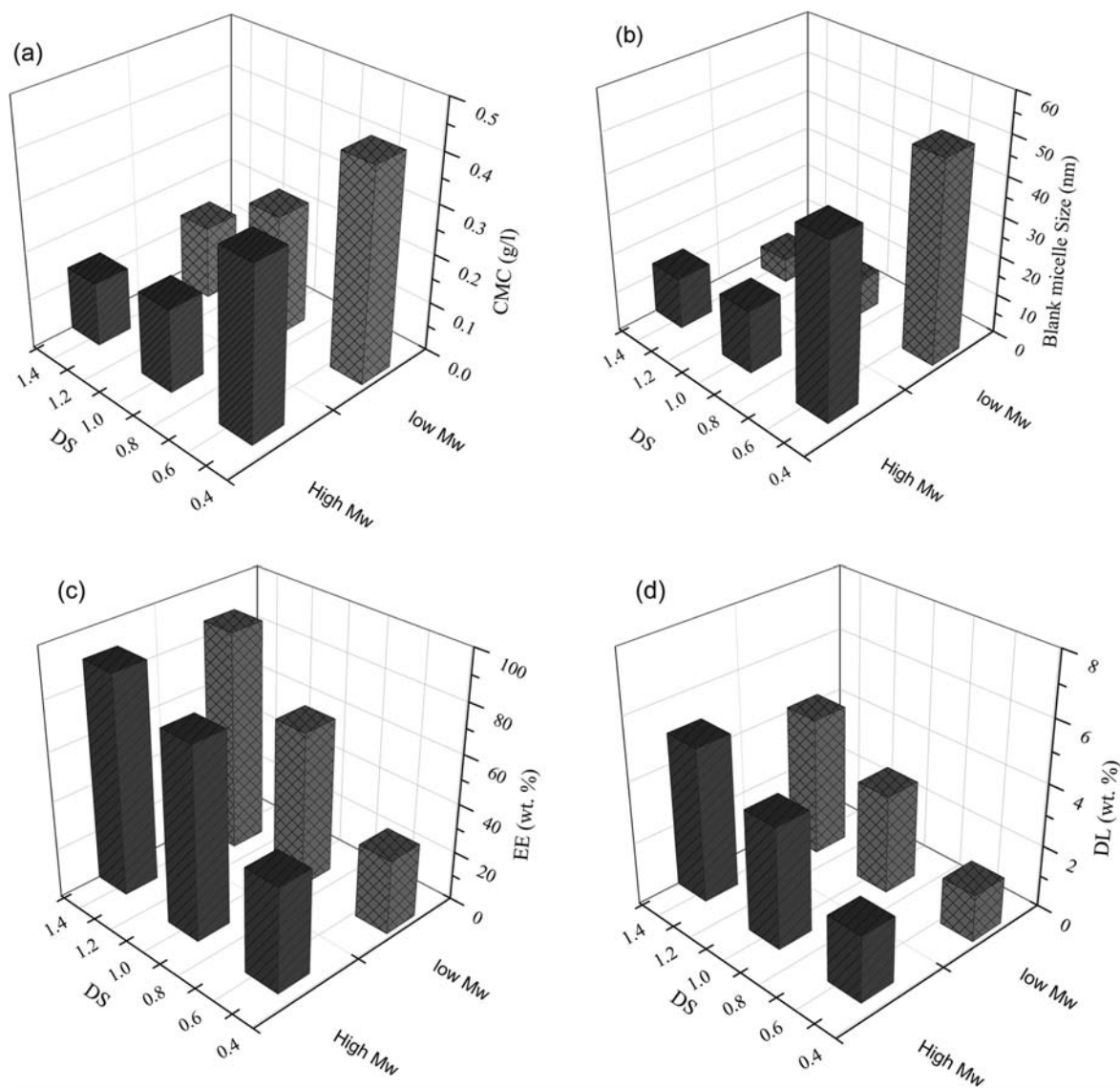
Figure 8. Effect of DS and M_w on the CMC (a), micelle size (b), drug encapsulation efficiency (EE %) (c), and DL % (d) of the MCC-g-PLA self-assembled micelles.

compositional parameters of PLA side chains such as DP_{PLA} and DS also showed the same trend with increase of the in-feed ratio of L-LA to cellulose. The MCC-g-PLA copolymers with DS of 0.55−2.0 were prepared when the molar ratio of AGU to L-LA was increased from 1:1 to 1:6. Furthermore, the MS, W_{PLA}, and DS decreased when the reaction temperature increased from 110 to 130 °C at the same molar ratio of AGU to L-LA, which indicated that higher reaction temperature was not beneficial to the reaction. However, the experimental conditions including the in-feed ratio of L-LA to cellulose and temperature did not have significant influence on the length of grafted side chain. Although regular changes were observed with varied experimental conditions, the values of DP_{PLA} are barely adjusted in a narrow range of 1.74−2.39.

GPC was employed to evaluate M_n, M_w, and M_w/M_n values of the MCC-g-PLA copolymers, and the results are depicted in Table 1. The results showed that M_w values of all copolymers ranged from 6 to 40 kDa, and the M_n and M_w values increased with increasing PLA content in copolymers. However, the polydispersity (M_w/M_n) was barely changed with the progressive increment of grafting chains. Moreover, it was

found that the reaction temperature had an obvious influence on the M_w of MCC-g-PLA copolymers prepared in ILs system. Taking MCC-g-PLA$_{0.50}$ and MCC-g-PLA$_{0.55}$ as examples, with all of the other conditions kept constant, when the reaction temperature was increased from 110 to 130 °C, the M_w of MCC-g-PLA products decreased from 50972 to 10844 Da. The other samples prepared at different temperatures (e.g., MCC-g-PLA$_{0.96}$ and MCC-g-PLA$_{0.99}$; MCC-g-PLA$_{1.37}$ and MCC-g-PLA$_{1.43}$) presented similar trends. This phenomenon was probably caused by degradation of the cellulose main chain at high temperature in ILs.

Physical Properties of MCC-g-PLA Copolymers with Various Molecular Factors. The solubility of MCC-g-PLA copolymers with various molecular factors in several representative solvents was evaluated, and the results are shown in Table 2. As shown, all of the obtained copolymers had good solubility in the common polar organic solvents such as DMSO and DMF. Additionally, all of the copolymers except for MCC-g-PLA$_{2.00}$ (DS = 2.00) had good solubility in water. These results suggested that the graft reaction successfully took place and that the hydrogen bonds and crystalline structure of

cellulose were disrupted after modification. However, when the less polar organic solvents such as hexane and THF were employed to dissolve the MCC-g-PLA copolymers, only slight swelling behaviors could be observed even with heating. This phenomenon was probably due to the polarity of the grafted PLA side chains.

To investigate the crystalline character of MCC-g-PLA copolymers, XRD experiments were performed with MCC and graft copolymers, as shown in Figure 4. MCC displayed a typical XRD pattern of cellulose I, with the main diffraction signals appearing at around 2θ of 14.90°, 16.67°, 22.82°, and 34.67°, normally corresponding to the diffraction planes of 101, 10$\bar{1}$, 002, and 040, respectively.[43] However, none of these crystallization peaks of cellulose was observed for the MCC-g-PLA copolymers, but instead there appeared one broad peak at 2θ of 20.0°, indicating the copolymers were amorphous. The XRD patterns of MCC-g-PLA copolymers with different DS values were very similar. Only a slight increase of the intensity of the peak at $2\theta = 20.0°$ was observed with increasing DS. The crystalline pattern of PLA grafted chains could not be observed in the spectra of all the copolymers due to its short chain length.

The thermal stability of MCC-g-PLA graft copolymers was studied by TGA in N_2 atmosphere, and the TG and DTG curves of MCC and graft copolymers are shown in Figure 5. It can be seen that the thermal stability of graft copolymers was not as good as MCC. The graft copolymers showed two decomposition stages and two maximum decomposition temperatures (T_{max}), whereas the MCC had only one maximum decomposition temperature. The T_{max1} of MCC-g-PLA copolymers corresponded to the scission of the PLA linkage from the cellulose backbone followed by the decomposition of the PLA grafts, and T_{max2} was ascribed to the decomposition of cellulose residues. The lower T_{max2} of MCC-g-PLA relative to cellulose confirmed the fact that the hydrogen bonds in cellulose had been partially destroyed by the introduction of PLA segments. From Figure 5, it could also be seen that the thermal stability of copolymers decreased with the increasing DS values of PLA side chains. This was because the thermal properties of PLA esters were not as stable as those of cellulose. Accordingly, it was concluded that the thermal stability of graft copolymers was correlated with the substitution degree of PLA grafting side chains.

Self-Assembly Behavior of MCC-g-PLA Copolymers. The self-assembly of amphiphilic copolymers in water is based on nonpolar and hydrophobic interactions between the lipophilic core-forming segments. The major driving force behind the self-association of amphiphilic polymers is a gain in entropy of the solvent molecules as the hydrophobic fragments withdraw from the aqueous surroundings with the formation of micelle core stabilized with hydrophilic segments exposed into water.[44] A dialysis method was taken in this study to prepare the self-assembled micelles of MCC-g-PLA copolymers. For this method, a water-miscible organic solvent (such as DMSO, DMF, acetone, or THF) that could dissolve both the copolymer and the drug was required, and the micellization was triggered with slow removal of the organic phase. The particle size and size distribution of the self-assembled micelles were determined by DLS, and the results are presented in Table 3. It could be found that the size of the MCC-g-PLA micelles varied in the range from 6 to 52 nm. The effect of molecular factors on the micelle size will be discussed in detail below. The morphology of the MCC-g-PLA micelles was

characterized by TEM (Figure 6). As shown in Figure 6, spherical nanosized micelles were formed from the self-assembly of MCC-g-PLA copolymers in aqueous solution.

The same as for the conventional surfactant, the self-assembly of amphiphilic polymer starts as the concentration of the polymer reaches the threshold concentration (CMC); thus, the CMC is an important parameter showing the self-assembly ability. The CMC values of MCC-g-PLA copolymers were determined by using the pyrene fluorescence probe technique. Pyrene is a molecular fluorescent probe with the intensity ratio of the first peak (375 nm) and the third peak (386 nm) I_1/I_3 in its emission spectrum very sensitive to the polarity of environment. When micelles formed, pyrene was preferentially located in the hydrophobic core of the micelle, and thus the microenvironment of pyrene changed from hydrophilic to hydrophobic. Accordingly, the fluorescence intensity ratio of I_1/I_3 would present an obvious change. One typical fluorescence spectrum of MCC-g-PLA copolymers with increasing polymer concentration is shown in Figure 7a. Figure 7b shows the intensity ratio (I_{375}/I_{386}) of the pyrene excitation spectra versus the log concentrations of MCC-g-PLA copolymer (MS = 3.17, DS = 1.43). On the basis of the crossover point of the plot curve, the CMC value of the copolymer (MCC-g-PLA$_{1.43}$) was calculated to be 0.13 mg/mL. Similarly, the fluorescence spectra of all the other MCC-g-PLA copolymers were taken, and the CMC values were calculated according to the same method.

Antitumor Drug Loading Capacity of MCC-g-PLA Micelles. The antitumor drug PTX had been demonstrated to have powerful antitumor ability against a wide spectrum of cancers, such as metastatic breast cancer, epithelial ovarian cancer, colon cancer, small and nonsmall cell lung cancer, and neck cancer.[45] However, serious disadvantages of PTX, for example, cytotoxicity and insolubility in water, had limited its clinical application.[39,46] Therefore, it is important to develop biocompatible carriers to assist solubilization and reduce side effects of PTX.[6,38,47] In this work, MCC-g-PLA self-assembled micelles were used as carriers for PTX. Practically, PTX dissolved in methanol was added into the MCC-g-PLA micelle solution followed by a 30 min ultrasonic treatment. It had been demonstrated that the process of solubilization of water-insoluble drugs by micelle-forming amphiphilic copolymers included two steps.[7] The initial solubilization proceeded via the displacement of solvent (water) molecules from the micelle core. In the following, the solubilized drug began to accumulate in the center of the micelle core while pushing hydrophobic segments away from this area. Extensive solubilization might result in the increase of micelle size due to the expansion of its core with solubilized drug. As shown in Table 3, the sizes of the PTX-loaded micelles (in the range of 97−167 nm) were obviously larger than the unloaded micelles (in the range of 7−51 nm), indicating that PTX had been incorporated into the MCC-g-PLA micelles effectively. Similar results were also observed in other studies.[1]

Effect of Polymer Architecture on the Self-Assembly and Drug Loading Properties of MCC-g-PLA Micelles. The self-assembly and drug loading properties of the MCC-g-PLA micelles were found to be strongly dependent on the copolymer's molecular factors, especially the DS and M_w of copolymers. Thus, the correlation between the molecular factors (DS and M_w) and MCC-g-PLA micelle properties is summarized in Figure 8. Figure 8a depicts the CMC values of MCC-g-PLA copolymers with different DS and M_w. It could be seen that the CMC of copolymers was not significantly affected

by M_w, but was strongly affected by DS. When the DS of the copolymers was increased from 0.55 to 1.43, the CMC was reduced from 0.35 to 0.13 g/L. In comparison, the particle size of MCC-g-PLA micelles was dependent on both the DS and M_w of copolymers. With the other parameters' being comparable, high M_w copolymers showed obviously larger micelle size. Moreover, the micelle size was reduced from 44 to 13 nm when the DS of the copolymers was increased from 0.55 to 1.43. Figure 8, panels c and d, presents the PTX loading capacity of the MCC-g-PLA micelles. As shown, the encapsulation efficiency (EE, %) of the MCC-g-PLA micelles was enhanced from 42.54 to 89.30% with increasing DS values of PLA from 0.55 to 1.43. Accordingly, the PTX loading content (DL, %) was increased from 2.13 to 4.97%. M_w values of copolymers also had some effect on their drug loading capacities. For the copolymers (such as MCC-g-PLA$_{0.96}$ and MCC-g-PLA$_{0.99}$) with comparable DS, the EE of the copolymer with high M_w was 78.02%, whereas the EE of the copolymer with low M_w was 63.76%. This was probably due to the larger micelle size of high M_w copolymers. Among all samples, MCC-g-PLLA$_{1.43}$ (MS = 4.78, DS = 1.43) showed the highest PTX loading ability with DL of 4.97% and EE as high as 89.30%.

In summary, a series of MCC-g-PLA amphiphilic copolymers were successfully synthesized by homogeneous ring-opening graft copolymerization of L-LA onto cellulose in a new ionic liquid, BmimCl. The results of FT-IR, ^{1}H NMR, ^{13}C NMR, and GPC analyses indicated that well-defined copolymers with specific graft length and favorable W_{PLA} contents of side chains were obtained. These MCC-g-PLA copolymers were able to form self-assembled spherical nanomicelles in aqueous solution, with the particle size and CMC values determined be 10−50 nm and 0.13−0.43 g/L, respectively. PTX as a model antitumor drug was easily encapsulated into the core of MCC-g-PLA micelles. The self-assembly and drug loading properties of the micelles were strongly dependent on the polymer architecture. Copolymers with higher DS of PLA had smaller CMC and micelle size, whereas copolymers with higher M_w had larger CMC and micelle size. Furthermore, the drug loading content and entrapment efficiency of PTX were increased with the progressive increment of PLA side chains and M_w of copolymers. With adequate control over the self-assembly and drug loading behaviors, these MCC-g-PLA amphiphilic copolymers prepared from all biocompatible, nontoxic, and biodegradable materials hold great promise for applications as antitumor drug carriers.

■ AUTHOR INFORMATION

Corresponding Author

*Phone/fax: +86 20 87111861. E-mail: (X.W.) fewangxh@scut.edu.cn or (R.-C.S.) ynsun@scut.edu.cn.

Notes

The authors declare no competing financial interest.

■ REFERENCES

(1) Hu, F. Q.; Liu, L. N.; Du, Y. Z.; Yuan, H. Synthesis and antitumor activity of doxorubicin conjugated stearic acid-g-chitosan oligosaccharide polymeric micelles. *Biomaterials* **2009**, *30*, 6955−6963.

(2) Yuan, H.; Lu, L. J.; Du, Y. Z.; Hu, F. Q. Stearic acid-g-chitosan polymeric micelle for oral drug delivery: in vitro transport and in vivo absorption. *Mol. Pharmaceutics* **2010**, *8*, 225−238.

(3) Yao, Z.; Zhang, C.; Ping, Q.; Yu, L. A series of novel chitosan derivatives: synthesis, characterization and micellar solubilization of paclitaxel. *Carbohydr. Polym.* **2007**, *68*, 781−792.

(4) Wang, H.; Zhao, Y.; Wu, Y.; Hu, Y. L.; Nan, K.; Nie, G.; Chen, H. Enhanced anti-tumor efficacy by co-delivery of doxorubicin and paclitaxel with amphiphilic methoxy PEG-PLGA copolymer nanoparticles. *Biomaterials* **2011**, *32*, 8281−8290.

(5) Song, N.; Liu, W.; Tu, Q.; Liu, R.; Zhang, Y.; Wang, J. Preparation and in vitro properties of redox-responsive polymeric nanoparticles for paclitaxel delivery. *Colloid Surf. B* **2011**, *87*, 454−463.

(6) Zhang, Y.; Huo, M.; Zhou, J.; Yu, D.; Wu, Y. Potential of amphiphilically modified low molecular weight chitosan as a novel carrier for hydrophobic anticancer drug: synthesis, characterization, micellization and cytotoxicity evaluation. *Carbohydr. Polym.* **2009**, *77*, 231−238.

(7) Hu, F. Q.; Ren, G. F.; Yuan, H.; Du, Y. Z.; Zeng, S. Shell cross-linked stearic acid grafted chitosan oligosaccharide self-aggregated micelles for controlled release of paclitaxel. *Colloid Surf. B* **2006**, *50*, 97−103.

(8) Topp, M. D. C.; Dijkstra, P. J.; Talsma, H.; Feijen, J. Thermosensitive micelle-forming block copolymers of poly(ethylene glycol) and poly(N-isopropylacrylamide). *Macromolecules* **1997**, *30*, 8518−8520.

(9) Benahmed, A.; Ranger, M.; Leroux, J. C. Novel polymeric micelles based on the amphiphilic diblock copolymer poly(N-vinyl-2-pyrrolidone)-*block*-poly(D,L-lactide). *Pharm. Res.* **2001**, *18*, 323−328.

(10) Saito, R.; Okamura, S. I.; Ishizu, K. Synthesis of poly(vinyl alcohol) core-polystyrene shell type microspheres. *Polymer* **1995**, *36*, 4515−4520.

(11) Calderara, F.; Riess, G. Characterization of polystyrene-*block*-poly(4-vinyl-pyridine) block copolymer micelles in toluene solution. *Macromol. Chem. Phys.* **1996**, *197*, 2115−2132.

(12) Yasugi, K.; Nagasaki, Y.; Kato, M.; Kataoka, K. Preparation and characterization of polymer micelles from poly(ethylene glycol)-poly(D,L-lactide) block copolymers as potential drug carrier. *J. Controlled Release* **1999**, *62*, 89−100.

(13) Park, E. K.; Kim, S. Y.; Lee, S. B.; Lee, Y. M. Folate-conjugated methoxy poly(ethylene glycol)/poly(ε-caprolactone) amphiphilic block copolymeric micelles for tumor-targeted drug delivery. *J. Controlled Release* **2005**, *109*, 158−168.

(14) Akagi, T.; Kaneko, T.; Kida, T.; Akashi, M. Preparation and characterization of biodegradable nanoparticles based on poly(γ-glutamic acid) with L-phenylalanine as a protein carrier. *J. Controlled Release* **2005**, *108*, 226−236.

(15) Chen, W.; Chen, H.; Hu, J.; Yang, W.; Wang, C. Synthesis and characterization of polyion complex micelles between poly(ethylene glycol)-grafted poly(aspartic acid) and cetyltrimethyl ammonium bromide. *Colloid Surf. A* **2006**, *278*, 60−66.

(16) Eccleston, M. E.; Williams, S. L.; Yue, Z.; Chen, R.; Lee, C. K.; Anikina, E.; Pawlyn, C.; Barrand, M. A.; Slater, N. K. H. Design and in-vitro testing of effective poly(L-lysine iso-phthalamide) based drug targeting systems for solid tumours. *Food Bioprod. Process.* **2005**, *83*, 141−146.

(17) Brown, M. D.; Schätzlein, A.; Brownlie, A.; Jack, V.; Wang, W.; Tetley, L.; Gray, A. I.; Uchegbu, I. F. Preliminary characterization of novel amino acid based polymeric vesicles as gene and drug delivery agents. *Bioconjugate Chem.* **2000**, *11*, 880−891.

(18) Liu, Z.; Jiao, Y.; Wang, Y.; Zhou, C.; Zhang, Z. Polysaccharides-based nanoparticles as drug delivery systems. *Adv. Drug Deliv. Rev.* **2008**, *60*, 1650−1662.

(19) Aouada, F. A.; De Moura, M. R.; Orts, W. J.; Mattoso, L. H. C. Preparation and characterization of novel micro- and nanocomposite

hydrogels containing cellulosic fibrils. *J. Agric. Food Chem.* **2011**, *59*, 9433−9442.

(20) Murray, B. S.; Durga, K.; De Groot, P. W. N.; Kakoulli, A.; Stoyanov, S. D. Preparation and characterization of the foam-stabilizing properties of cellulose−ethyl cellulose complexes for use in foods. *J. Agric. Food Chem.* **2011**, *59*, 13277−13288.

(21) Gupta, K. C.; Khandekar, K. Temperature-responsive cellulose by ceric(IV) ion-initiated graft copolymerization of *N*-isopropylacrylamide. *Biomacromolecules* **2003**, *4*, 758−765.

(22) Meng, T.; Gao, X.; Zhang, J.; Yuan, J.; Zhang, Y.; He, J. Graft copolymers prepared by atom transfer radical polymerization (ATRP) from cellulose. *Polymer* **2009**, *50*, 447−454.

(23) Shen, D.; Huang, Y. The synthesis of CDA-*g*-PMMA copolymers through atom transfer radical polymerization. *Polymer* **2004**, *45*, 7091−7097.

(24) Sui, X.; Yuan, J.; Zhou, M.; Zhang, J.; Yang, H.; Yuan, W.; Wei, Y.; Pan, C. Synthesis of cellulose-*graft*-poly(*N*,*N*-dimethylamino-2-ethyl methacrylate) copolymers via homogeneous ATRP and their aggregates in aqueous media. *Biomacromolecules* **2008**, *9*, 2615−2620.

(25) Teramoto, Y.; Nishio, Y. Biodegradable cellulose diacetate-*graft*-poly(L-lactide)s: thermal treatment effect on the development of supramolecular structures. *Biomacromolecules* **2003**, *5*, 397−406.

(26) Jiang, C.; Wang, X.; Sun, P.; Yang, C. Synthesis and solution behavior of poly(ε-caprolactone) grafted hydroxyethyl cellulose copolymers. *Int. J. Biol. Macromol.* **2011**, *48*, 210−214.

(27) Zhu, J.; Wang, W. T.; Wang, X. L.; Li, B.; Wang, Y. Z. Green synthesis of a novel biodegradable copolymer base on cellulose and poly(*p*-dioxanone) in ionic liquid. *Carbohydr. Polym.* **2009**, *76*, 139−144.

(28) Teramoto, Y.; Nishio, Y. Cellulose diacetate-*graft*-poly(lactic acid)s: synthesis of wide-ranging compositions and their thermal and mechanical properties. *Polymer* **2003**, *44*, 2701−2709.

(29) Yuan, W.; Yuan, J.; Zhang, F.; Xie, X. Syntheses, characterization, and in vitro degradation of ethyl cellulose-*graft*-poly(ε-caprolactone)-*block*-poly(L-lactide) copolymers by sequential ring-opening polymerization. *Biomacromolecules* **2007**, *8*, 1101−1108.

(30) Chen, D.; Sun, B. New tissue engineering material copolymers of derivatives of cellulose and lactide: their synthesis and characterization. *Mater. Sci. Eng., C* **2000**, *11*, 57−60.

(31) Buchanan, C. M.; Dorschel, D.; Gardner, R. M.; Komarek, R. J.; Matosky, A. J.; White, A. W.; Wood, M. D. The influence of degree of substitution on blend miscibility and biodegradation of cellulose acetate blends. *J. Polym. Environ.* **1996**, *4*, 179−195.

(32) Yan, C.; Zhang, J.; Lv, Y.; Yu, J.; Wu, J.; Zhang, J.; He, J. Thermoplastic cellulose-*graft*-poly(L-lactide) copolymers homogeneously synthesized in an ionic liquid with 4-dimethylaminopyridine catalyst. *Biomacromolecules* **2009**, *10*, 2013−2018.

(33) Hao, Y.; Peng, J.; Li, J.; Zhai, M.; Wei, G. An ionic liquid as reaction media for radiation-induced grafting of thermosensitive poly(*N*-isopropylacrylamide) onto microcrystalline cellulose. *Carbohydr. Polym.* **2009**, *77*, 779−784.

(34) Xu, Q.; Kennedy, J. F.; Liu, L. An ionic liquid as reaction media in the ring opening graft polymerization of ε-caprolactone onto starch granules. *Carbohydr. Polym.* **2008**, *72*, 113−121.

(35) Heinze, T.; Schwikal, K.; Barthel, S. Ionic liquids as reaction medium in cellulose functionalization. *Macromol. Biosci.* **2005**, *5*, 520−525.

(36) Zhang, H.; Wu, J.; Zhang, J.; He, J. 1-Allyl-3-methylimidazolium chloride room temperature ionic liquid: a new and powerful nonderivatizing solvent for cellulose. *Macromolecules* **2005**, *38*, 8272−8277.

(37) Dong, H.; Xu, Q.; Li, Y.; Mo, S.; Cai, S.; Liu, L. The synthesis of biodegradable graft copolymer cellulose-*graft*-poly(L-lactide) and the study of its controlled drug release. *Colloid Surf. B* **2008**, *66*, 26−33.

(38) Wang, F.; Zhang, D.; Zhang, Q.; Chen, Y.; Zheng, D.; Hao, L.; Duan, C.; Jia, L.; Liu, G.; Liu, Y. Synergistic effect of folate-mediated targeting and verapamil-mediated P-gp inhibition with paclitaxel-polymer micelles to overcome multi-drug resistance. *Biomaterials* **2011**, *32*, 9444−9456.

(39) Wang, Y. S.; Jiang, Q.; Li, R. S.; Liu, L. L.; Zhang, Q. Q.; Wang, Y. M.; Zhao, J. Self-assembled nanoparticles of cholesterol-modified *O*-carboxymethyl chitosan as a novel carrier for paclitaxel. *Nanotechnology* **2008**, *19*, 145101.

(40) Pinkert, A.; Marsh, K. N.; Pang, S.; Staiger, M. P. Ionic liquids and their interaction with cellulose. *Chem. Rev.* **2009**, *109*, 6712−6728.

(41) Qiu, L.; Bae, Y. Polymer architecture and drug delivery. *Pharm. Res.* **2006**, *23*, 1−30.

(42) Zhu, J.; Dong, X. T.; Wang, X. L.; Wang, Y. Z. Preparation and properties of a novel biodegradable ethyl cellulose grafting copolymer with poly(*p*-dioxanone) side-chains. *Carbohydr. Polym.* **2010**, *80*, 350−359.

(43) Cao, Y.; Tan, H. Structural characterization of cellulose with enzymatic treatment. *J. Mol. Struct.* **2004**, *705*, 189−193.

(44) Gaucher, G.; Dufresne, M.-H.; Sant, V. P.; Kang, N.; Maysinger, D.; Leroux, J. C. Block copolymer micelles: preparation, characterization and application in drug delivery. *J. Controlled Release* **2005**, *109*, 169−188.

(45) Mo, R.; Jin, X.; Li, N.; Ju, C.; Sun, M.; Zhang, C.; Ping, Q. The mechanism of enhancement on oral absorption of paclitaxel by *N*-octyl-*O*-sulfate chitosan micelles. *Biomaterials* **2011**, *32*, 4609−4620.

(46) Lee, J.; Lee, S. C.; Acharya, G.; Chang, C.-J.; Park, K. Hydrotropic solubilization of paclitaxel: analysis of chemical structures for hydrotropic property. *Pharm. Res.* **2003**, *20*, 1022−1030.

(47) Shan, L.; Cui, S.; Du, C.; Wan, S.; Qian, Z.; Achilefu, S.; Gu, Y. A paclitaxel-conjugated adenovirus vector for targeted drug delivery for tumor therapy. *Biomaterials* **2012**, *33*, 146−162.